# Electric quadrupole transitions in carbon dioxide

Cite as: J. Chem. Phys. 154, 211104 (2021); doi: 10.1063/5.0053279
Submitted: 6 April 2021 • Accepted: 18 May 2021 •
Published Online: 3 June 2021

**Andrey Yachmenev,**[1,2,a)] **Alain Campargue,**[3,b)] **Sergei N. Yurchenko,**[4,c)] **Jochen Küpper,**[1,2,5]
**and Jonathan Tennyson**[4]

## AFFILIATIONS

[1] Center for Free-Electron Laser Science, Deutsches Elektronen-Synchrotron DESY, Notkestraße 85, 22607 Hamburg, Germany
[2] Center for Ultrafast Imaging, Universität Hamburg, Luruper Chaussee 149, 22761 Hamburg, Germany
[3] Univ. Grenoble Alpes, CNRS, LIPhy, 38000 Grenoble, France
[4] Department of Physics and Astronomy, University College London, London WC1E 6BT, United Kingdom
[5] Department of Physics, Universität Hamburg, Luruper Chaussee 149, 22761 Hamburg, Germany

[a)] **Author to whom correspondence should be addressed:** andrey.yachmenev@cfel.de
[b)] **Electronic mail:** alain.campargue@univ-grenoble-alpes.fr
[c)] **Electronic mail:** s.yurchenko@ucl.ac.uk

## ABSTRACT

Recent advances in high sensitivity spectroscopy have made it possible, in combination with accurate theoretical predictions, to observe, for the first time, very weak electric quadrupole transitions in a polar polyatomic molecule of water. Here, we present accurate theoretical predictions of the complete quadrupole rovibrational spectrum of a non-polar molecule $CO_2$, important in atmospheric and astrophysical applications. Our predictions are validated by recent cavity enhanced absorption spectroscopy measurements and are used to assign few weak features in the recent ExoMars Atmospheric Chemistry Suite mid-infrared spectroscopic observations of the Martian atmosphere. Predicted quadrupole transitions appear in some of the mid-infrared $CO_2$ and water vapor transparency regions, making them important for detection and characterization of the minor absorbers in water- and $CO_2$-rich environments, such as those present in the atmospheres of Earth, Venus, and Mars.

The intensities of electric quadrupole (E2) transitions are known to be very weak, six to eight orders of magnitude smaller than the intensities of electric dipole (E1) transitions. Until very recently, the E2 transitions were measured only in non-polar or slightly polar diatomics, such as $H_2$,[1–6] $O_2$,[7,8] $N_2$,[9–13] HD,[14] and $N_2^+$,[15] i.e., molecules that otherwise do not exhibit E1 transitions or, as regards HD, they are extremely weak. In polar molecules, with polyatomics being considerably richer in the number and density of rovibrational transitions, strong E1 absorption profiles blanket most of the weak features in the rovibrational spectrum.

Tracing and assigning weak spectral features as belonging to the E1 transitions of minor isotopologues or other meager molecular species, or, indeed, the E2 or magnetic dipole (M1) transitions of the main molecular constituent, can be endlessly intricate and, hence, can benefit from precise theoretical predictions. So far as there were no reliable calculations of the E2 and magnetic dipole M1 transitions for polyatomic molecules, detection of these electric-dipole-forbidden features and investigation of their seemingly surreptitious role in high-resolution spectroscopy remain unexplored.

The role of weak rovibrational transitions in the spectrum of carbon dioxide ($CO_2$) is fundamental to monitoring its isotopic composition in the atmosphere for the understanding of carbon cycle processes,[16–19] and it is becoming increasingly precise for the determination of new gas signatures in $CO_2$-rich planetary atmospheres, such as Mars and Venus. To this end, the completeness of spectroscopic data for the main isotopologue $^{12}C^{16}O_2$ is crucial, especially in its transparency windows, to reduce the likelihood of its weak spectroscopic features being mistakenly assigned to those of minor isotopologues or other less-abundant molecular species.[20,21] For example, recently discovered weak M1 transitions of $CO_2$ in the spectrum of the Martian atmosphere[21] would not be known as belonging to $CO_2$ without the accurate knowledge of the E1 transitions of its main and minor isotopologues. While there have been multiple and still ongoing computational and experimental efforts to fully characterize the E1 spectra of major isotopologues of $CO_2$,[22–24] the contributions from the dipole-forbidden E2 and, until very recently, M1[21] transitions have not had the slightest attention.

In this Communications, we report the first complete and accurate E2 line list for carbon dioxide $^{12}C^{16}O_2$, which was validated in the 3.3 $\mu$m transparency window by recent laboratory measurements using Optical-Feedback-Cavity Enhanced Absorption Spectroscopy (OFCEAS).[25] Based on our predictions and laboratory measurements, we report a detection of the E2 lines in the Martian atmospheric spectra recorded by using the ExoMars Trace Gas Orbiter Atmospheric Chemistry Suite (ACS) instrument.[26] We also present our newly developed variational computational methodology, which is capable of high-accuracy predictions of the E2 spectra for arbitrary polar molecules.

Our computational approach is based on the general variational approach TROVE,[27–30] which, for triatomic molecules, employs an exact kinetic energy operator.[31] For $CO_2$, an accurate empirically refined potential energy surface (PES) "Ames-2" was employed.[32] In TROVE, the vibrational basis set is constructed in a multi-step procedure from contracted and symmetry-adapted products of one-dimensional basis sets, each represented by solutions $\chi_n(q)$ ($n = 0, 1, 2 \ldots$) of the one-dimensional Schrödinger equation for a selected vibrational mode $q$.[29] For $CO_2$, there are two stretching and one bending vibrational modes, with the respective quantum numbers $n_1$, $n_2$, and $n_3$. Since $CO_2$ is linear, its bending vibration is coupled to a molecular rotational motion about the linearity axis, which is the molecular $z$ axis. For this reason, the bending basis functions cannot be fully decoupled from the molecular rotation and parametrically depend on the rotational quantum number $K$ of the $\hat{J}_z$ angular momentum operator, hence the notation $n_3^{(K)}$. We refer to Ref. 31 for the details of treatment of linear and quasi-linear molecules. The size of vibrational basis was controlled by the condition $2(n_1 + n_2) + n_3^{(K)} \le 64$.

The full rovibrational basis set is constructed as a symmetrized product of the symmetry-adapted vibrational basis functions $\psi_{\lambda,K}^{(\Gamma_{\rm vib})}$ and symmetry-adapted rigid-rotor wave functions $|J, K, \Gamma_{\rm rot}\rangle$,

$$\Psi_{\lambda,K}^{(J,\Gamma)} = \left\{\psi_{\lambda,K}^{(\Gamma_{\rm vib})} \times |J, K, \Gamma_{\rm rot}\rangle\right\}^{\Gamma}. \tag{1}$$

Here, $\lambda$ denotes a set of vibrational state quantum numbers and $\Gamma_{\rm vib}$, $\Gamma_{\rm rot}$, and $\Gamma$ denote the symmetries of the vibrational, rotational, and total wave functions, respectively. For $CO_2$, we employed the $\mathbf{C}_{2v}(M)$ molecular symmetry group. The total wavefunction for a rovibrational state $l$, with the quantum number of the total angular momentum $J$ and the total symmetry $\Gamma$, is a linear combination of rovibrational basis set functions,

$$\Phi_l^{(J,\Gamma)} = \sum_{K,\lambda} c_{K,\lambda}^{(J,\Gamma,l)} \Psi_{\lambda,K}^{(J,\Gamma)}, \tag{2}$$

where the linear expansion coefficients $c_{K,\lambda}^{(J,\Gamma,l)}$ are obtained by solving an eigenvalue problem with the full rovibrational Hamiltonian. All energies and eigenfunctions up to $J = 40$ were generated and used to produce the E2 line list for $CO_2$.

The achieved accuracy of energy level predictions for $CO_2$ is best characterized by the root-mean-square (rms) deviation of 0.06 cm$^{-1}$ between the calculated and experimental[33] rovibrational term values, evaluated across 337 band centers with energies up to 15 500 cm$^{-1}$ above the zero-point level. Considering the weakness of the E2 lines, the line position accuracy is crucial for discriminating them from the weak E1 lines of minor isotopologues and possible impurities. Further improvement of accuracy would require yet another round of empirical adjustment of the underlying PES, which is an inordinately expensive procedure. As a call for more practical solution, very often the variationally computed energies, providing that they are close enough to the experiment, are replaced by the corresponding experimentally determined values. The latter can be extracted from the experimental spectroscopic line positions using advanced combination difference techniques, such as MARVEL (Measured Active Rotational–Vibrational Energy Levels)[34–37] and RITZ (Rydberg–Ritz combination principle).[38,39] For $CO_2$, we used the experimental energy levels from the carbon dioxide spectroscopic databank[40] produced from a global effective Hamiltonian modeling of an exhaustive set of position measurements available in the literature.[41] More details about the computational procedure employed here and validation of its accuracy are presented in a study of the E1 line list of $CO_2$.[24]

The quadrupole spectrum was simulated using the variational approach RichMol,[42,43] a computer program designed for calculations of molecular rovibrational dynamics in the presence of an external electromagnetic field. The transition probability from an initial rovibrational state $|i\rangle = \Phi_l^{(J,\Gamma)}$ into a final state $|f\rangle = \Phi_{l'}^{(J',\Gamma')}$ due to the interaction of light with the quadrupole moment of the molecule is given by

$$P(f \leftarrow i) = g_{\rm ns}(2J' + 1)(2J + 1)\left|\mathcal{K}^{(J',\Gamma',l',J,\Gamma,l)}\right|^2, \tag{3}$$

where

$$\begin{aligned}\mathcal{K}^{(J',\Gamma',l',J,\Gamma,l)} = {} & \sum_{K'\lambda'}\sum_{K\lambda}\left[c_{K',\lambda'}^{(J',\Gamma',l')}\right]^* c_{K,\lambda}^{(J,\Gamma,l)} \\ & \times (-1)^{K'}\sum_{\sigma=-2}^{2}\begin{pmatrix} J & 2 & J' \\ K & \sigma & -K' \end{pmatrix} \\ & \times \sum_{\alpha,\beta=x,y,z} U_{\sigma,\alpha\beta}\langle\psi_{\lambda',K'}|Q_{\alpha,\beta}|\psi_{\lambda,K}\rangle.\end{aligned} \tag{4}$$

Here, $Q_{\alpha,\beta}$ denotes the traceless quadrupole moment tensor in the molecular frame and the matrix $U_{\sigma,\alpha\beta}$ transforms the quadrupole tensor from the Cartesian to spherical-tensor form [see, e.g., Eqs. (5-41)–(5-44) in Ref. 44]. The nuclear spin statistical factors $g_{\rm ns}$ for $^{12}C^{16}O_2$ are equal to 1 for initial state symmetries $A_1$ and $A_2$ and 0 otherwise.

The quadrupole moment tensor with elements as functions of internal coordinates is required to compute the vibrational expectation values $\langle\psi_{\lambda',K'}|Q_{\alpha,\beta}|\psi_{\lambda,K}\rangle$ in Eq. (4). A three-dimensional mesh of internal coordinates of $CO_2$ was used, containing about 2000 different nuclear geometries and covering the energy range of up to $hc \cdot 40\,000$ cm$^{-1}$ above the equilibrium energy. The quadrupole tensor at each point was computed using the all-electron coupled-cluster singles and doubles with perturbative triples [CCSD(T)] method in conjunction with the aug-cc-pwCVQZ basis set[45–47] and analytic gradient approach.[48] The electronic structure calculations employed the quantum chemistry package CFOUR.[49] For a molecular frame selected such that the $x$ axis bisects the valence bond angle

O–C–O and plane of the molecule for bent $CO_2$ is aligned with the $xz$ plane, the three non-zero elements of the quadrupole tensor $Q_{xx}$, $Q_{zz}$, and $Q_{xz}$ have the $A_1$, $A_1$, and $B_2$ symmetries, respectively. These were parameterized using fourth order symmetry-adapted power series expansions through least-squares fittings to the electronic structure data, with $\sigma_{\mathrm{rms}} < 10^{-4}$ a.u.

Our results for the quadrupole moment of $CO_2$ $Q^{\mathrm{e}}_{zz} = -3.1666$ a.u. $= -14.207 \times 10^{-40}$ C m$^2$ at the equilibrium $r_{\mathrm{e}} = 1.1614$ Å and its zero-point vibrational average $Q^{\mathrm{ZPVA}}_{zz} = -3.1627$ a.u. $= -14.190 \times 10^{-40}$ C m$^2$ agree very well with experimental data and previous calculations listed in Table I.

The line intensity of quadrupole transition in units cm/molecule is given by

$$I(f \leftarrow i) = \frac{4\pi^5 \nu^3 e^{-\beta E_l^{(J,\Gamma)}}\left(1 - e^{-\beta hc\nu}\right)}{(4\pi\epsilon_0)5hcZ(T)} P(f \leftarrow i), \qquad (5)$$

where $\nu = (E_{l'}^{(J',\Gamma')} - E_l^{(J,\Gamma)})/hc$ is the frequency of transition between lower $E_l^{(J,\Gamma)}$ and upper $E_{l'}^{(J',\Gamma')}$ state energies, $Z(T)$ is the partition function, and $\beta = 1/(kT)$. For $^{12}C^{16}O_2$, we used an accurate computed value of $Z(296\,\mathrm{K}) = 286.094$.[22] The computed quadrupole line list is provided in the supplementary material.

In Fig. 1(a), the calculated E2 line list for the main isotopologue, $^{12}C^{16}O_2$, is superimposed on the E1 line list of natural $CO_2$.[33] Both spectra are generated at room temperature, $T = 296$ K. The E1 lines of the minor isotopologues at natural abundances are plotted with cyan color. In general, the E2 bands are 6–8 orders of magnitude weaker than the E1 bands. The most prominent E2 band with line intensities of a few $10^{-29}$ cm/molecule is the bending plus anti-symmetric stretching $\nu_2 + \nu_3$ band at 3000 cm$^{-1}$ (3.3 $\mu$m), highlighted in Fig. 1(b).

**TABLE I.** Experimental and theoretical permanent electric quadrupole moments of $CO_2$ in $10^{-40}$ C m$^2$.

| Method | Value | Source |
|---|---|---|
| | *Experiment* | |
| Buckingham effect[a] | − 14.98 ± 0.50 | 50 |
| Buckingham effect[a] | −14.3 ± 0.6 | 51 |
| Buckingham effect[a] | −14.31 ± 0.74 | 52 |
| Cotton–Mouton effect[b] | −14.0 ± 0.7 | 53 |
| Collision-induced absorption | −14.9 ± 0.7 | 54 |
| Dielectric measurements | −14.94 ± 1.0 | 55 |
| | *Theory* | |
| CCSD(T)/CBS[c] | −14.22 ± 0.09 | 56 |
| CCSD(T)/CBS+ZPVC[d] | −14.29 ± 0.09 | 56 |
| CCSD(T)/6s4p4d1f | −14.3 | 57 |
| CCSD(T)/AwCVQZ | −14.207 | This work |
| CCSD(T)/AwCVQZ/ZPVC[d] | −14.190 | This work |

[a] Electric field gradient induced birefringence measurements.
[b] Magnetic field induced birefringence measurements.
[c] Complete basis set limit extrapolation with the additive core-valence correlation effect.
[d] Results corrected with the zero-point vibration.

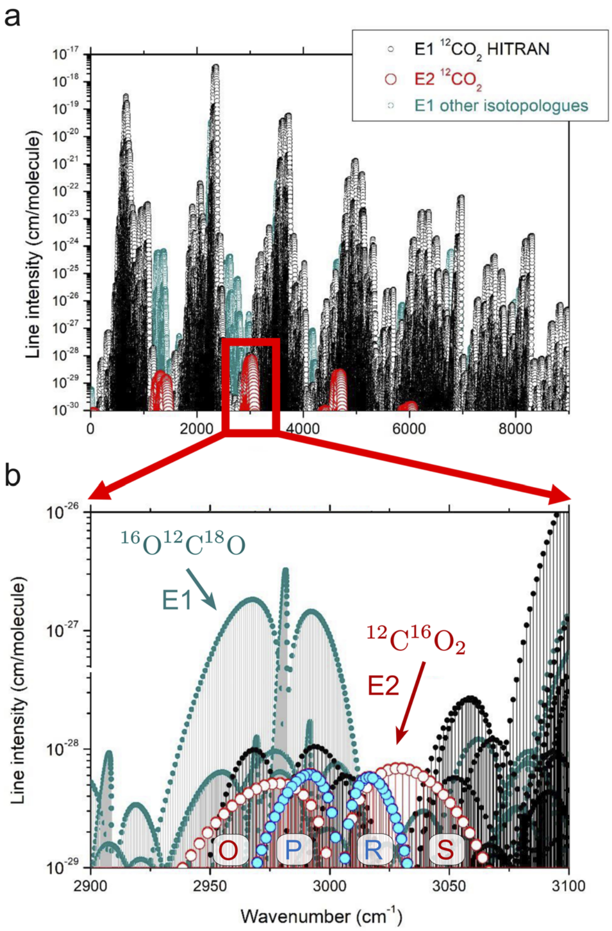

**FIG. 1.** (a) Overview of the calculated quadrupole spectrum of $^{12}C^{16}O_2$ (red) superimposed with its dipole spectrum (black) and the dipole spectrum of minor isotopologues (cyan). The spectra are generated for temperature $T = 296$ K. (b) A zoom into the $\nu_2 + \nu_3$ band, where the E2 transitions of $^{12}C^{16}O_2$ can be distinguished by larger circles, the $P$ and $R$ branches are plotted with cyan color, and $O$ and $S$ are branches plotted with red color.

In contrast with the E2 spectrum of water,[58,59] the E2 lines of $CO_2$ appear largely in the E1 transparency regions, which makes them possible to be observed. The reason for this is different approximate selection rules for the E1 and E2 transitions in $CO_2$ and in linear molecules, in general. For example, the $\nu_1$ and $\nu_2 + \nu_3$ E1 band transitions at 6.9 and 3.3 $\mu$m are dipole forbidden and, therefore, very weak. These bands are, however, directly allowed for the E2 transition mechanism, even in the rigid-rotor approximation.

As already mentioned, the E1 lines of the minor isotopologues of $CO_2$ make an important contribution to the transparency windows (see Fig. 1), where they overlap with the E2 lines of the main isotopologue. Indeed, the predicted $\nu_2 + \nu_3$ E2 band of $^{12}C^{16}O_2$ is almost entirely superimposed with the $\nu_2 + \nu_3$ E1 band of $^{16}O^{12}C^{18}O$, which is stronger by about a factor of 20, despite a natural isotopic abundance of only $4 \times 10^{-3}$. It should be noted that

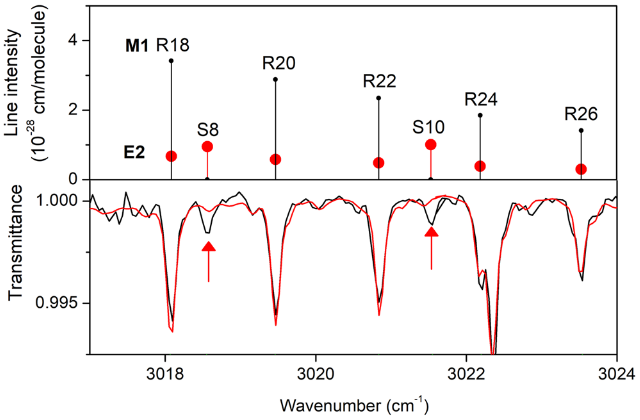

**FIG. 2.** Comparison of the ACS MIR transmission spectra of the atmosphere of Mars[21] near 3020 cm$^{-1}$ with the calculated line lists of the M1 and E2 $\nu_2 + \nu_3$ bands of $^{12}C^{16}O_2$. Upper panel: The presently calculated E2 transitions with *ab initio* intensities (red stems) are superimposed to the M1 transitions with intensities calculated in Ref. 61 (black stems). Lower panel: The ACS MIR spectrum (red line) with a best-fit synthetic model containing the contributions of the E1 bands of $CO_2$ and $H_2O$ based on the HITRAN 2016 database and of the M1 lines identified in Ref. 21. The assignments of the newly detected S8 and S10 E2 transitions are marked with red arrows.

due to the different symmetry, the $\nu_2 + \nu_3$ E1 band is allowed in $^{16}O^{12}C^{18}O$ but forbidden in $^{12}C^{16}O_2$.

The $\nu_2 + \nu_3$ band of $CO_2$ has recently been observed in the spectrum of Mars' atmosphere,[21] as recorded by using the ExoMars Trace Gas Orbiter ACS MIR (Atmospheric Chemistry Suite Mid-InfraRed) spectrometer. The recorded spectra (partly reproduced in Fig. 3) show strong intensity features that are more specific for M1 rather than the E2 transitions,[60] although no first-principles simulations for the M1 spectrum had been done. In particular, the presence of the strong *Q*-branch, which is very weak for the E2 band, see Fig. 1(b), and the absence of nearly as intense *O*- and *S*-branches argue for a dominant M1 mechanism.[60] However, this does not exclude the presence of the E2 features in the Martian spectrum, although, obviously, they must be less pronounced. Note that very recently, the dominant M1 $\nu_2 + \nu_3$ band was also detected in the laboratory from long path absorption measurements of $^{12}C^{16}O_2$ by Fourier transform spectroscopy (FTS).[61] These measurements indicated that the M1 line intensities estimated from the Martian spectrum[21] were overestimated by about a factor of 2. The effective dipole moment derived from a fit of the measured FTS intensities was used to calculate the line intensities displayed in Fig. 2.

As can be seen from Fig. 1(b), E2 transitions in the *O*-branch overlap completely with much stronger and generally broader E1 lines of $CO_2$ and, hence, are hardly discernible. A number of the *S*-branch transitions appear in a narrow region free from any strong E1 lines, which are thus possible to be observed. In Fig. 2, we compare our predicted *S*-branch transitions near 3020 cm$^{-1}$ to the ACS MIR transmission spectra displayed in Fig. 4 of Ref. 21. A clear position coincidence of the predicted *S*(8) and *S*(12) lines with unknown weak absorption features can be observed in the region 3018–3025 cm$^{-1}$.

A very recent laboratory study, dedicated to the measurements of the weak spectral features in the *S*-branch of the $\nu_2 + \nu_3$ band of $CO_2$ by OFCEAS,[25] has confirmed the strong M1 features originally observed in Martian $CO_2$. The measurements have also revealed a number of new features that can be assigned, by comparison with the theoretical line list, to the S12, S14, and S16 E2 lines, shown in Fig. 3. Notably, the intensities of the E2 *R*-branch transitions contribute to about 10%–15% of those of the dominant M1 features.

Intensity considerations provide further evidence supporting the detection of E2 lines in both ACS MIR and OFCEAS spectra. The intensity of the S8 and S10 E2 lines can be estimated from the Martian spectrum by comparison to the nearby R18–R22 for which line intensities are known from FTS laboratory spectra of Ref. 61. From a multi-line profile fit of the ACS MIR spectrum, the areas of the S8 and S10 lines were derived and scaled according to the absolute intensities of the nearby R18–R22 M1 lines.[61] We obtain 7.0 and 6.5 $\times 10^{-29}$ cm/molecule at 172 K for the absolute intensities of S8 and S10, which are in satisfactory agreement with our theoretically predicted values of 9.5 and 10.0 $\times 10^{-29}$ cm/molecule, respectively. As regards the S12, S14, and S16 lines observed in the OFCEAS spectra (Fig. 3), their intensities (and pressure broadening coefficients) were reported in Ref. 25. The OFCEAS intensities are also close to their predicted values, although showing a difference on the order of 30%, slightly larger than the estimated OFCEAS uncertainty.

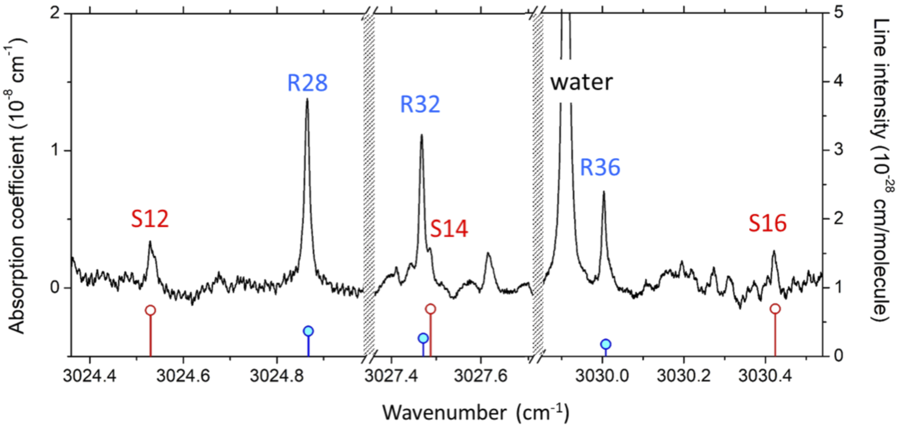

**FIG. 3.** Comparison of the laboratory spectrum of $CO_2$ at 60 mbar recorded by OFCEAS[25] with the calculated E2 line list of $^{12}C^{16}O_2$ in three spectral intervals of the E2 $\nu_2 + \nu_3$ band. The *R*- and *S*-band E2 transitions are plotted with blue and red stems, respectively. The S12, S14, and S16 E2 lines are apparent. The line intensities of the R28, R32, and R36 transitions are mostly due to the M1 transitions.

The experience of *ab initio* E2 intensity calculations for polyatomic molecules is very limited. Based on the wealth of the E1 experimental and theoretical investigations, it is nowadays normal to expect a 10%–20% error (for stronger bands) from *ab initio* predictions of electric dipole intensities using standard levels of theory, as in this work [CCSD(T)/aug-cc-pwCVQZ]. However, the electric quadrupole calculations are still unexplored territory. According to the current work, our prediction of the two E2 lines from $\nu_2 + \nu_3$ amounts to a 30% (overestimated) error in intensities at $T = 172$ K. In fact, a similar quality of the *ab initio* intensities was reported for the $\nu_1 + \nu_3$ E2 transitions of water in Ref. 58, which varied between 8% and 90% underestimating the experimental intensities. More work is needed, both experimental and theoretical, to establish the quality of the modern *ab initio* methods for the E2 intensities.

In summary, we presented an accurate computational methodology for calculating the electric quadrupole spectra of polyatomic molecules with the arbitrary structure. The calculated quadrupole transitions of $CO_2$ were confirmed by the high sensitivity spectroscopic measurements[25] with few of them newly identified in the spectrum of Mars' atmosphere. The quadrupole transitions are typically a million times weaker than the electric dipole transitions. The accurate characterization of the quadrupole transitions for the main atmospheric absorbers, especially in the mid-infrared transparency windows, will eliminate the misassignment of spectral features and thus help in precise detection of the minor atmospheric constituents. Being particularly sensitive to steeply varying fields, which are common in nature at the molecule–molecule and molecule–surface interfaces,[62–64] the electric quadrupole transitions can potentially be used for remote sensing of local molecular environments.

See the supplementary material for a quadrupole line list for $CO_2$ in the HITRAN-like format computed at $T = 296$ K with the threshold of $10^{-36}$ cm/molecule for the absorption coefficient. The rovibrational states were assigned using the HITRAN quantum-number convention for $CO_2$ (see Ref. 65). The ExoMol diet[66] scheme of $CO_2$ was used for the broadening coefficients (air and self), while the line shifts were set to zero.

We thank Trokhimovskiy for providing the original ACS MIR transmission spectra of the atmosphere of Mars.

This work was supported by the STFC (Project No. ST/R000476/1) and the ERC Advanced Grant (Project No. 883830). The authors acknowledge the use of the UCL Legion High Performance Computing Facility (Legion@UCL) and associated support services in the completion of this work, along with the Cambridge Service for Data Driven Discovery (CSD3), part of which is operated by the University of Cambridge Research Computing on behalf of the STFC DiRAC HPC Facility (www.dirac.ac.uk). The DiRAC component of CSD3 was funded by BEIS capital funding via STFC capital, Grant Nos. ST/P002307/1 and ST/R002452/1, and STFC operations, Grant No. ST/R00689X/1. DiRAC is part of the National e-Infrastructure. This work was further supported by the Deutsche Forschungsgemeinschaft (DFG) through the Cluster of Excellence "Advanced Imaging of Matter" (AIM, EXC 2056, ID 390715994). We acknowledge support by Deutsches Elektronen-Synchrotron DESY, a member of the Helmholtz Association (HGF), and the use of the Maxwell computational resources operated at Deutsches Elektronen-Synchrotron DESY.

## DATA AVAILABILITY

The data that support the findings of this study are available within the article and its supplementary material.

## REFERENCES

[1] G. Herzberg, "Quadrupole rotation-vibration spectrum of the hydrogen molecule," Nature **163**, 170 (1949).

[2] A. Goldman, J. Reid, and L. S. Rothman, "Identification of electric quadrupole $O_2$ and $N_2$ lines in the infrared atmospheric absorption spectrum due to the vibration-rotation fundamentals," Geophys. Res. Lett. **8**, 77, https://doi.org/10.1029/gl008i001p00077 (1981).

[3] D. Reuter, D. E. Jennings, and J. W. Brault, "The $v = 1 \leftarrow 0$ quadrupole spectrum of $N_2$," J. Mol. Spectrosc. **115**, 294 (1986).

[4] K. H. Baines, M. E. Mickelson, L. E. Larson, and D. W. Ferguson, "The abundances of methane and *ortho*/*para* hydrogen on Uranus and Neptune: Implications of new laboratory 4-0 $H_2$ quadrupole line parameters," Icarus **114**, 328 (1995).

[5] A. Campargue, S. Kassi, K. Pachucki, and J. Komasa, "The absorption spectrum of $H_2$: CRDS measurements of the (2-0) band, review of the literature data and accurate *ab initio* line list up to 35 000 $cm^{-1}$," Phys. Chem. Chem. Phys. **14**, 802 (2012).

[6] S.-M. Hu, H. Pan, C.-F. Cheng, Y. R. Sun, X.-F. Li, J. Wang, A. Campargue, and A.-W. Liu, "The $v = 3 \leftarrow 0$ $S(0)$–$S(3)$ electric quadrupole transitions of $H_2$ near 0.8 $\mu$m," Astrophys. J. **749**, 76 (2012).

[7] H. Naus, A. de Lange, and W. Ubachs, "$b^1\Sigma_g^+ - X^3\Sigma_g^-$(0,0) band of oxygen isotopomers in relation to tests of the symmetrization postulate in $^{16}O_2$," Phys. Rev. A **56**, 4755 (1997).

[8] D. A. Long, D. K. Havey, M. Okumura, H. M. Pickett, C. E. Miller, and J. T. Hodges, "Laboratory measurements and theoretical calculations of $O_2$ *A* band electric quadrupole transitions," Phys. Rev. A **80**, 042513 (2009).

[9] J. Reid, R. L. Sinclair, A. M. Robinson, and A. R. W. McKellar, "Observation of electric quadrupole transitions in the fundamental band of $O_2$ in the 1600 $cm^{-1}$ region," Phys. Rev. A **24**, 1944 (1981).

[10] L. S. Rothman and A. Goldman, "Infrared electric quadrupole transitions of atmospheric oxygen," Appl. Opt. **20**, 2182 (1981).

[11] S. Kassi and A. Campargue, "Cavity ring down spectroscopy with $5 \times 10^{-13}$ $cm^{-1}$ sensitivity," J. Chem. Phys. **137**, 234201 (2012).

[12] S. Kassi, I. E. Gordon, and A. Campargue, "First detection of transitions in the second quadrupole overtone band of nitrogen near 1.44 $\mu$m by CW-CRDS with $6 \times 10^{-13}$ $cm^{-1}$ sensitivity," Chem. Phys. Lett. **582**, 6 (2013).

[13] P. Čermák, S. Vasilchenko, D. Mondelain, S. Kassi, and A. Campargue, "First laboratory detection of an absorption line of the first overtone electric quadrupolar band of $N_2$ by CRDS near 2.2 $\mu$m," Chem. Phys. Lett. **668**, 90 (2017).

[14] S. Vasilchenko, D. Mondelain, S. Kassi, P. Čermák, B. Chomet, A. Garnache, S. Denet, V. Lecocq, and A. Campargue, "The HD spectrum near 2.3 $\mu$m by CRDS-VECSEL: Electric quadrupole transition and collision-induced absorption," J. Mol. Spectrosc. **326**, 9 (2016).

[15] M. Germann, X. Tong, and S. Willitsch, "Observation of electric-dipole-forbidden infrared transitions in cold molecular ions," Nat. Phys. **10**, 820 (2014).

[16] W. G. Mook, M. Koopmans, A. F. Carter, and C. D. Keeling, "Seasonal, latitudinal, and secular variations in the abundance and isotopic ratios of atmospheric carbon dioxide: 1. Results from land stations," J. Geophys. Res.: Oceans **88**, 10915, https://doi.org/10.1029/jc088ic15p10915 (1983).

[17] E. Kerstel and H. Meijer, "Optical isotope ratio measurements in hydrology," in *Isotopes in the Water Cycle: Past, Present and Future of a Developing Science*, edited by P. K. Aggarwal, J. R. Gat, and K. F. Froehlich (Springer Netherlands, Dordrecht, 2005), pp. 109–123.

[18] H. D. Graven, "Impact of fossil fuel emissions on atmospheric radiocarbon and various applications of radiocarbon over this century," Proc. Natl. Acad. Sci. U. S. A. **112**, 9542 (2015).

[19] J. Lelieveld, K. Klingmüller, A. Pozzer, R. T. Burnett, A. Haines, and V. Ramanathan, "Effects of fossil fuel and total anthropogenic emission removal on public health and climate," Proc. Natl. Acad. Sci. U. S. A. **116**, 7192 (2019).

[20] A. D. McCartt, T. Ognibene, G. Bench, and K. Turteltaub, "Measurements of carbon-14 with cavity ring-down spectroscopy," Nucl. Instrum. Methods Phys. Res., Sect. B **361**, 277 (2015).

[21] A. Trokhimovskiy, V. Perevalov, O. Korablev, A. A. Fedorova, K. S. Olsen, J.-L. Bertaux, A. Patrakeev, A. Shakun, F. Montmessin, F. Lefèvre, and A. Lukashevskaya, "First observation of the magnetic dipole $CO_2$ main isotopologue absorption band at 3.3 $\mu$m in the atmosphere of Mars by the ExoMars Trace Gas Orbiter ACS instrument," Astron. Astrophys. **639**, A142 (2020).

[22] E. J. Zak, J. Tennyson, O. L. Polyansky, L. Lodi, N. F. Zobov, S. A. Tashkun, and V. I. Perevalov, "Room temperature line lists for $CO_2$ asymmetric isotopologues with *ab initio* computed intensities," J. Quant. Spectrosc. Radiat. Transfer **203**, 265 (2017).

[23] T. Odintsova, E. Fasci, L. Moretti, E. J. Zak, O. L. Polyansky, J. Tennyson, L. Gianfrani, and A. Castrillo, "Highly-accurate intensity factors of pure $CO_2$ lines near 2 $\mu$m," J. Chem. Phys. **146**, 244309 (2017).

[24] S. N. Yurchenko, T. M. Mellor, R. S. Freedman, and J. Tennyson, "ExoMol line lists XXXIX. Ro-vibrational molecular line list for $CO_2$," Mon. Not. R. Astron. Soc. **496**, 5282 (2020).

[25] H. Fleurbaey, R. Grilli, D. Mondelain, S. Kassi, A. Yachmenev, S. N. Yurchenko, and A. Campargue, "Electric-quadrupole and magnetic-dipole contributions to the $\nu_2 + \nu_3$ band of carbon dioxide near 3.3 $\mu$m," J. Quant. Spectrosc. Radiat. Transfer **266**, 107558 (2021).

[26] O. I. Korablev, D. A. Belyaev, Y. S. Dobrolenskiy, A. Y. Trokhimovskiy, and Y. K. Kalinnikov, "Acousto-optic tunable filter spectrometers in space missions (invited)," Appl. Opt. **57**, C103 (2018).

[27] S. N. Yurchenko, W. Thiel, and P. Jensen, "Theoretical ROVibrational energies (TROVE): A robust numerical approach to the calculation of rovibrational energies for polyatomic molecules," J. Mol. Spectrosc. **245**, 126 (2007).

[28] A. Yachmenev and S. N. Yurchenko, "Automatic differentiation method for numerical construction of the rotational-vibrational Hamiltonian as a power series in the curvilinear internal coordinates using the Eckart frame," J. Chem. Phys. **143**, 014105 (2015).

[29] S. N. Yurchenko, A. Yachmenev, and R. I. Ovsyannikov, "Symmetry adapted ro-vibrational basis functions for variational nuclear motion: TROVE approach," J. Chem. Theory Comput. **13**, 4368 (2017).

[30] K. L. Chubb, A. Yachmenev, J. Tennyson, and S. N. Yurchenko, "Treating linear molecule HCCH in calculations of rotation-vibration spectra," J. Chem. Phys. **149**, 014101 (2018).

[31] S. N. Yurchenko and T. M. Mellor, "Treating linear molecule $XY_2$ in calculations of rotation-vibration spectra," J. Chem. Phys. **153**, 154106 (2020).

[32] X. Huang, D. W. Schwenke, R. S. Freedman, and T. J. Lee, "Ames-2016 line lists for 13 isotopologues of $CO_2$: Updates, consistency, and remaining issues," J. Quant. Spectrosc. Radiat. Transfer **203**, 224 (2017).

[33] I. E. Gordon *et al.*, "The HITRAN2016 molecular spectroscopic database," J. Quant. Spectrosc. Radiat. Transfer **203**, 3 (2017).

[34] T. Furtenbacher, A. G. Császár, and J. Tennyson, "MARVEL: Measured active rotational–vibrational energy levels," J. Mol. Spectrosc. **245**, 115 (2007).

[35] A. G. Császár, G. Czakó, T. Furtenbacher, and E. Mátyus, "An active database approach to complete rotational–vibrational spectra of small molecules," Annu. Rep. Comput. Chem. **3**, 155 (2007).

[36] T. Furtenbacher and A. G. Császár, "The role of intensities in determining characteristics of spectroscopic networks," J. Mol. Struct.: THEOCHEM **1009**, 123 (2012).

[37] R. Tóbiás, T. Furtenbacher, J. Tennyson, and A. G. Császár, "Accurate empirical rovibrational energies and transitions of $H_2{}^{16}O$," Phys. Chem. Chem. Phys. **21**, 3473 (2019).

[38] S. Mikhailenko, S. Tashkun, T. Putilova, E. Starikova, L. Daumont, A. Jenouvrier, S. Fally, M. Carleer, C. Hermans, and A. Vandaele, "Critical evaluation of measured rotation–vibration transitions and an experimental dataset of energy levels of $HD^{18}O$," J. Quant. Spectrosc. Radiat. Transfer **110**, 597 (2009).

[39] S. Tashkun, T. Velichko, and S. Mikhailenko, "Critical evaluation of measured pure-rotation and rotation-vibration line positions and an experimental dataset of energy levels of $^{12}C^{16}O$ in $X^1\Sigma^+$ state," J. Quant. Spectrosc. Radiat. Transfer **111**, 1106 (2010), Special Issue Dedicated to Laurence S. Rothman on the Occasion of his 70th Birthday.

[40] S. A. Tashkun, V. I. Perevalov, R. R. Gamache, and J. Lamouroux, "CDSD-296, high resolution carbon dioxide spectroscopic databank: Version for atmospheric applications," J. Quant. Spectrosc. Radiat. Transfer **152**, 45 (2015).

[41] S. A. Tashkun, V. I. Perevalov, J. L. Teffo, L. S. Rothman, and V. Tyuterev, "Global fitting of $^{12}C^{16}O_2$ vibrational–rotational line positions using the effective Hamiltonian approach," J. Quant. Spectrosc. Radiat. Transfer **60**, 785 (1998).

[42] A. Owens and A. Yachmenev, "RichMol: A general variational approach for rovibrational molecular dynamics in external electric fields," J. Chem. Phys. **148**, 124102 (2018).

[43] A. Yachmenev, L. V. Thesing, and J. Küpper, "Laser-induced dynamics of molecules with strong nuclear quadrupole coupling," J. Chem. Phys. **151**, 244118 (2019); arXiv:1910.13275 [physics].

[44] R. N. Zare, *Angular Momentum: Understanding Spatial Aspects in Chemistry and Physics*, 1st ed. (Wiley, 1988).

[45] T. H. Dunning, "Gaussian basis sets for use in correlated molecular calculations. I. The atoms boron through neon and hydrogen," J. Chem. Phys. **90**, 1007 (1989).

[46] R. A. Kendall, T. H. Dunning, and R. J. Harrison, "Electron affinities of the first-row atoms revisited. Systematic basis sets and wave functions," J. Chem. Phys. **96**, 6796 (1992).

[47] K. A. Peterson and T. H. Dunning, "Accurate correlation consistent basis sets for molecular core–valence correlation effects: The second row atoms Al–Ar, and the first row atoms B–Ne revisited," J. Chem. Phys. **117**, 10548 (2002).

[48] G. E. Scuseria, "Analytic evaluation of energy gradients for the singles and doubles coupled cluster method including perturbative triple excitations: Theory and applications to FOOF and $Cr_2$," J. Chem. Phys. **94**, 442 (1991).

[49] J. Stanton, J. Gauss, M. Harding *et al.*, CFOUR, a quantum chemical program package written by J. F. Stanton, J. Gauss, M. E. Harding, and P. G. Szalay, with contributions from A. A. Auer, R. J. Bartlett, U. Benedikt, C. Berger, D. E. Bernholdt, Y. J. Bomble, L. Cheng, O. Christiansen, M. Heckert, O. Heun, C. Huber, T.-C. Jagau, D. Jonsson, J. Jusélius, K. Klein, W. J. Lauderdale, D. A. Matthews, T. Metzroth, L. A. Mück, D. P. O'Neill, D. R. Price, E. Prochnow, C. Puzzarini, K. Ruud, F. Schiffmann, W. Schwalbach, S. Stopkowicz, A. Tajti, J. Vázquez, F. Wang, and J. D. Watts, the integral packages MOLECULE, J. Almlöf and P. R. Taylor, PROPS, P. R. Taylor, ABACUS, T. Helgaker, H. J. Aa. Jensen, P. Jørgensen, and J. Olsen, and ECP routines by A. V. Mitin and C. van Wüllen, for the current version, see http://www.cfour.de, 2019.

[50] M. Battaglia, A. Buckingham, D. Neumark, R. Pierens, and J. Williams, "The quadrupole moments of carbon dioxide and carbon disulphide," Mol. Phys. **43**, 1015 (1981).

[51] J. N. Watson, I. E. Craven, and G. L. Ritchie, "Temperature dependence of electric field-gradient induced birefringence in carbon dioxide and carbon disulfide," Chem. Phys. Lett. **274**, 1 (1997).

[52] N. Chetty and V. Couling, "Measurement of the electric quadrupole moments of $CO_2$ and OCS," Mol. Phys. **109**, 655 (2011).

[53] H. Kling and W. Hüttner, "The temperature dependence of the Cotton-Mouton effect of $N_2$, CO, $N_2O$, $CO_2$, OCS, and $CS_2$ in the gaseous state," Chem. Phys. **90**, 207 (1984).

[54] W. Ho, G. Birnbaum, and A. Rosenberg, "Far-infrared collision-induced absorption in $CO_2$. I. Temperature dependence," J. Chem. Phys. **55**, 1028 (1971).

[55] A. Hourri, J. M. St-Arnaud, and T. K. Bose, "Dielectric and pressure virial coefficients of imperfect gases: $CO_2$–$SF_6$ mixtures," J. Chem. Phys. **106**, 1780 (1997).

[56] S. Coriani, A. Halkier, A. Rizzo, and K. Ruud, "On the molecular electric quadrupole moment and the electric-field-gradient-induced birefringence of $CO_2$ and $CS_2$," Chem. Phys. Lett. **326**, 269 (2000).

[57] G. Maroulis, "Electric (hyper)polarizability derivatives for the symmetric stretching of carbon dioxide," Chem. Phys. **291**, 81 (2003).

[58] A. Campargue, S. Kassi, A. Yachmenev, A. A. Kyuberis, J. Küpper, and S. N. Yurchenko, "Observation of electric-quadrupole infrared transitions in water vapor," Phys. Rev. Res. **2**, 023091 (2020).

[59] A. Campargue, A. M. Solodov, A. A. Solodov, A. Yachmenev, and S. N. Yurchenko, "Detection of electric-quadrupole transitions in water vapour near 5.4 and 2.5 $\mu$m," Phys. Chem. Chem. Phys. **22**, 12476 (2020).

[60] V. Perevalov, A. Y. Trokhimovskiy, A. Lukashevskaya, O. Korablev, A. Fedorova, and F. Montmessin, "Magnetic dipole and electric quadrupole absorption in carbon dioxide," J. Quant. Spectrosc. Radiat. Transfer **259**, 107408 (2021).

[61] Y. Borkov, A. Solodov, A. Solodov, and V. Perevalov, "Line intensities of the 01111–00001 magnetic dipole absorption band of $^{12}C^{16}O_2$: Laboratory measurements," J. Mol. Spectrosc. **376**, 111418 (2021).

[62] T. Karman, M. A. J. Koenis, A. Banerjee, D. H. Parker, I. E. Gordon, A. van der Avoird, W. J. van der Zande, and G. C. Groenenboom, "$O_2$–$O_2$ and $O_2$–$N_2$ collision-induced absorption mechanisms unravelled," Nat. Chem. **10**, 549 (2018).

[63] E. Rusak, J. Straubel, P. Gładysz, M. Göddel, A. Kedziorski, M. Kühn, F. Weigend, C. Rockstuhl, and K. Słowik, "Enhancement of and interference among higher order multipole transitions in molecules near a plasmonic nanoantenna," Nat. Commun. **10**, 5775 (2019).

[64] J. Mun and J. Rho, "Importance of higher-order multipole transitions on chiral nearfield interactions," Nanophotonics **8**, 46 (2019).

[65] L. S. Rothman and L. D. Young, "Infrared energy levels and intensities of carbon dioxide-II," J. Quant. Spectrosc. Radiat. Transf. **25**, 505 (1981).

[66] E. J. Barton, C. Hill, M. Czurylo, H.-Y. Li, A. Hyslop, S. N. Yurchenko, and J. Tennyson, "The ExoMol diet of line-by-line pressure-broadening parameters," J. Quant. Spectrosc. Radiat. Transfer **203**, 490 (2017).